© 2017. Published by The Company of Biologists Ltd | Development (2017) 144, 3042-3053 doi:10.1242/dev.153239

STEM CELLS AND REGENERATION

RESEARCH ARTICLE

Morphogen and community effects determine cell fates in response to BMP4 signaling in human embryonic stem cells

Anastasiia Nemashkalo[1], Albert Ruzo[2], Idse Heemskerk[1] and Aryeh Warmflash[1,3,*]

ABSTRACT

Paracrine signals maintain developmental states and create cell fate patterns *in vivo* and influence differentiation outcomes in human embryonic stem cells (hESCs) *in vitro*. Systematic investigation of morphogen signaling is hampered by the difficulty of disentangling endogenous signaling from experimentally applied ligands. Here, we grow hESCs in micropatterned colonies of 1-8 cells ('µColonies') to quantitatively investigate paracrine signaling and the response to external stimuli. We examine BMP4-mediated differentiation in µColonies and standard culture conditions and find that in µColonies, above a threshold concentration, BMP4 gives rise to only a single cell fate, contrary to its role as a morphogen in other developmental systems. Under standard culture conditions BMP4 acts as a morphogen but this requires secondary signals and particular cell densities. We find that a 'community effect' enforces a common fate within µColonies, both in the state of pluripotency and when cells are differentiated, and that this effect allows a more precise response to external signals. Using live cell imaging to correlate signaling histories with cell fates, we demonstrate that interactions between neighbors result in sustained, homogenous signaling necessary for differentiation.

KEY WORDS: Human embryonic stem cells, Micropatterning, BMP4 pathway, Differentiation mechanisms

INTRODUCTION

Morphogen signaling pathways control cell fate during embryonic development and can be manipulated to produce particular fate outcomes in human embryonic stem cells (hESCs). During development, all signals both originate from, and are received by, the cells of the embryo; however, cultured cells combine extrinsic influences from the culture medium with endogenous signals passed between cells. In hESCs, secondary signals often perturb the outcome of directed differentiation (Kurek et al., 2015; Warmflash et al., 2014; Yu et al., 2011). Whether endogenous signals are required to maintain particular states, such as the pluripotent state, or to ensure the robustness of differentiation into coherent territories has not been investigated in hESCs. Dissecting the effects of paracrine signals from responses to external stimuli would enable researchers to harness endogenous signals to achieve particular aims, and aid in dissecting the role of these signals in the developing embryo.

The BMP pathway is a conserved morphogen signaling pathway that regulates dorsal-ventral patterning in species from flies to mammals (Bier and De Robertis, 2015) and has also been shown to be essential for mammalian gastrulation (Arnold and Robertson, 2009; Winnier et al., 1995). However, the difficulty in obtaining quantitative data has prevented determining whether BMP functions as a morphogen during mammalian gastrulation. Interestingly, in hESCs, there is increasing evidence that treatment with BMP4 leads to trophoectodermal (Horii et al., 2016; Li et al., 2013; Xu et al., 2002) and mesodermal (Kurek et al., 2015; Warmflash et al., 2014; Yu et al., 2011) fates, and that the mesodermal fates may be lost when Wnt, Nodal or FGF signaling is inhibited. Although there is abundant molecular data supporting the identity of these hESC-derived trophoectodermal cells, it has remained controversial (reviewed by Li and Parast, 2014) because the correlates of hESCs, the cells of the epiblast, do not give rise to trophoectodermal lineages, and data showing that hESC-derived trophoectoderm cells can function *in vivo* are also lacking. In light of this controversy, we will refer to these cells as 'trophoectoderm-like' cells.

When colony geometries are controlled, BMP4 can trigger the formation of patterns containing trophectoderm-like cells and all three embryonic germ layers (Etoc et al., 2016; Warmflash et al., 2014). These patterns arise in response to homogeneous treatment with BMP4 because of secondary paracrine signals that are required for producing and positioning the mesendodermal territories (Warmflash et al., 2014). Under these culture conditions, in which cells are housed within large colonies, it is difficult to disentangle the direct response to the BMP signal from the effects of interactions between the cells (Bernardo et al., 2011). It is therefore unclear whether the different fates induced by BMP4 treatment depend on the dose of BMP4 and, if so, whether cells directly read the BMP4 concentration. Quantitative dissection of the cellular response to supplied BMP4, as well as any paracrine interactions that function in the state of pluripotency or during BMP4-mediated differentiation, could resolve these important issues.

Here we use a micropatterning approach to isolate the effects of BMP treatment from the secondary endogenous signals that are active both in the state of pluripotency and during BMP-mediated differentiation. We confined cells to very small colonies ranging from 1 to 8 cells (referred to as 'µColonies'), allowing us to compare isolated cells, which respond only to the exogenous signaling, with cells housed within increasing large colonies where the contribution of paracrine signaling increases. Our results show that, in this context, BMP4 does not act as a morphogen but instead functions as a switch and, above a threshold, induces only the trophectoderm-like fate. By contrast, in standard culture conditions, in which colonies may consist of hundreds or thousands of cells, BMP4 elicits both mesodermal and trophectoderm-like fates in a dose-dependent manner that also requires Nodal signaling and particular cell densities. Further, we find that the main effect of secondary signals within µColonies is to enforce a common fate within the colony. This enforcement allows cells to more faithfully remain pluripotent in conditions supporting this state and to differentiate

[1]Department of Biosciences, Rice University, Houston, TX 77005, USA. [2]Laboratory of Stem Cell Biology and Molecular Embryology, The Rockefeller University, New York, NY 10065, USA. [3]Department of Bioengineering, Rice University, Houston, TX 77005, USA.

*Author for correspondence (aryeh.warmflash@rice.edu)

A.W., 0000-0002-5679-2268

Received 9 April 2017; Accepted 20 July 2017

 Development (2017) 144, 3042-3053 doi:10.1242/dev.153239

sensitively and homogenously in response to external stimuli. We show that this enforcement is the result of more sustained BMP signaling in larger μColonies, and that in standard culture conditions the outcome of BMP-mediated differentiation correlates with the duration of the BMP signal rather than the initial response.

RESULTS

BMP4 produces nearly pure populations of trophectoderm-like cells in μColonies

We first optimized cell seeding such that nearly all μColonies contain between 1 and 8 cells (Fig. 1A,B). Cells in μColonies grown for 42 h in the pluripotency-supporting medium MEF-CM expressed the pluripotency markers SOX2, OCT4 (POU5F1) and NANOG (Fig. S1A-C). In the experiments described below, we used SOX2 protein expression levels as a marker for hESC pluripotency but show that NANOG obeys similar trends (Fig. S2). We next assayed the response of μColonies to a range of BMP4 concentrations (0.1-30 ng/ml) for 42 h.

In response to increasing BMP4 levels, cells within μColonies transitioned from pluripotent ($SOX2^{+}$) to a differentiated fate expressing CDX2 and GATA3 and lacking expression of brachyury (BRA, or T), SOX17, EOMES, NANOG and SOX2 (Fig. S1D,E, Fig. 1C). Consistent with a growing body of literature on BMP4-mediated differentiation (Horii et al., 2016; Li and Parast, 2014; Xu et al., 2002), we identify these cells as trophectoderm-like, and we subsequently used CDX2 as a marker for this fate. Besides CDX2 and GATA3, all other differentiation markers were detected in less than 2% of cells in the population, and in all conditions nearly the entire population of cells expressed either the SOX2 marker of pluripotency or the CDX2 differentiation marker. We detected almost no BRA^{+} cells at any dose (Fig. 1C). BMP4 doses of 0.1-0.3 ng/ml produced mixtures of $SOX2^{+}$ and $CDX2^{+}$ cells, whereas 1 ng/ml or higher yielded nearly pure $CDX2^{+}$ populations with complete downregulation of SOX2 expression (Fig. 1D). By contrast, previous literature has shown that larger colonies differentiate to a heterogeneous mixture of fates even in response to

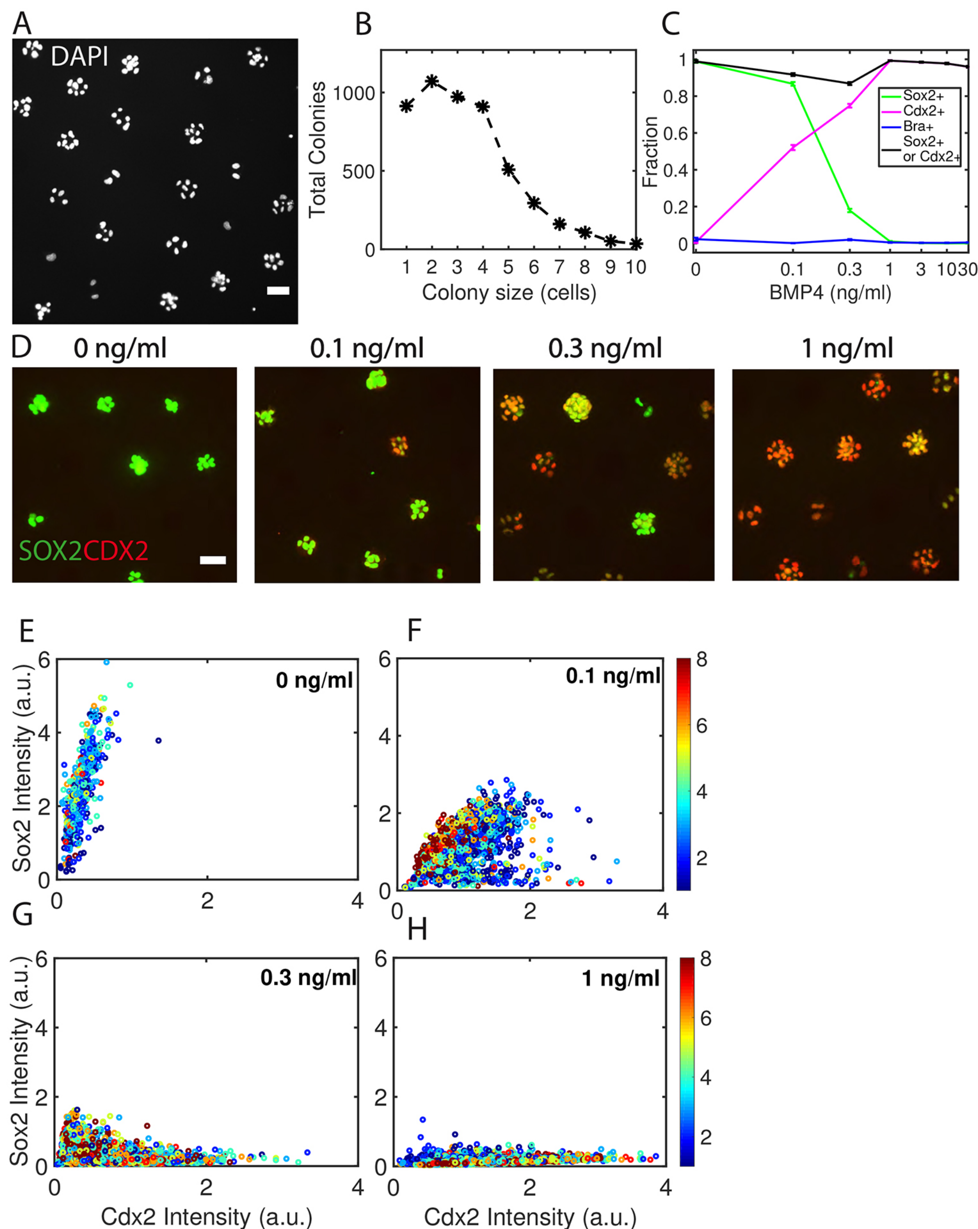

Fig. 1. BMP causes differentiation of μColonies to a single fate with a sharp threshold. (A) Representative image of hESCs grown in μColonies for 42 h. (B) Representative distribution of colony sizes after 42 h of culture. (C) Fractions of $SOX2^{+}$, $CDX2^{+}$ or BRA^{+} cells upon differentiation with BMP4 for 42 h. (D) Example images of immunofluorescence for CDX2 and SOX2 at the indicated BMP4 doses. (E-H) Scatter plots of SOX2 versus CDX2 markers for the indicated BMP4 concentrations. Each dot corresponds to a single cell, and the color code indicates the size of the colony containing that cell. Scale bars: 50 μm. See also Figs S1 and S2. Experiments on dose response to BMP4 in μColonies were performed twice.

 Development (2017) 144, 3042-3053 doi:10.1242/dev.153239

much higher doses of BMP4 (Tang et al., 2012; Warmflash et al., 2014). These results establish that cells in μColonies differentiate more sensitively and homogenously than cells in standard-size colonies in response to BMP4 ligand, and suggest that arrays of small colonies, like those we employ here, might have utility in directed differentiation schemes.

In standard culture, BMP elicits a morphogen effect that depends on Nodal signaling and cell density

To better understand the lack of mesodermal differentiation in μColonies, we compared the differentiation outcomes in response to a similar range of BMP4 doses for cells grown without confinement to small colonies. We used the pan-mesodermal and primitive streak marker BRA to determine the extent of mesodermal differentiation. We seeded cells such that the density was homogenous throughout the culture dish and varied this density (see below). We observed a morphogen effect in that the cell fate depended on the concentration of BMP4: below 2 ng/ml BMP4, cells remained in the SOX2$^+$ pluripotent state; at 2-4 ng/ml, cells differentiated to BRA$^+$ mesodermal cells, reaching a maximum of ~30% BRA$^+$ cells with the remainder CDX2$^+$; while at higher doses cells primarily adopted a CDX2$^+$ BRA$^-$ trophoectoderm-like fate (Fig. 2A top, Fig. 2B, Fig. S3A-C).

If cells directly read the BMP4 concentration, inhibitors of other signaling pathways should not perturb the morphogen effect. We found that treatment with the Activin/Nodal signaling inhibitor SB431542 abolished mesoderm differentiation at all doses, so that cells switched between only the SOX2$^+$ and CDX2$^+$ fates as in μColonies (Fig. 2A bottom, Fig. 2C, Fig. S3D). This supports the idea that the morphogen effect in response to BMP4 requires secondary signals. We reasoned that the response to secondary signals should be density dependent, and examined the role of cell density in differentiation outcomes. Indeed, at the dose of peak BRA induction (2 ng/ml) we only observed BRA expression at seeding densities of 30×10^3 and 60×10^3 cells/cm^2 but not at lower or higher densities (Fig. 2D, Fig. S3E). At higher BMP4 doses, cells did not express BRA at any cell density but primarily expressed CDX2 at low cell densities and SOX2 at high cell densities (Fig. 2E, Fig. S3F). Note that at both 2 and 10 ng/ml BMP4 at high densities, cells failed to differentiate and remained SOX2$^+$, consistent with other reports that BMP signaling and differentiation are inhibited at high cell densities (Etoc et al., 2016). Finally, to explicitly confirm that activating the Activin/Nodal pathway together with BMP stimulation would be sufficient to give rise to mesodermal differentiation, we compared μColonies treated with BMP4 and Activin with those treated with BMP4 alone. Consistent with the above results, we observed substantial mesodermal differentiation in colonies treated with BMP4 and Activin but not in those treated with BMP4 alone (Fig. S4). Thus, taken together, our results support a model in which only the CDX2$^+$ fate is a direct consequence of BMP4 signaling. Mesodermal differentiation can also occur at particular doses, but it requires secondary signaling through the Activin/Nodal pathway, and is only induced at particular cell densities. In μColonies treated with BMP4 alone, cell numbers are likely to be too low to produce sufficient secondary Nodal signals to induce mesodermal fates, but these can be induced by adding Activin to the medium.

A community effect enforces a common fate within μColonies in both the pluripotent and differentiation states

We noted that in the μColony experiments above, even at BMP4 concentrations that produced mixtures of different fates (CDX2$^+$ or SOX2$^+$), the fates of cells within an individual colony were highly correlated, whereas neighboring colonies often differed in fate, suggesting reinforcement of a common fate within the μColony (Fig. 1D), a phenomenon referred to as the ‘community effect’ (Bolouri and Davidson, 2010; Gurdon, 1988). To investigate whether a community effect is operating within μColonies, we examined the expression of the SOX2 and CDX2 markers as a function of the number of cells in the colony at varying BMP4 doses. Interestingly, under pluripotency-supporting conditions, expression of the pluripotency marker SOX2 increased with colony size, whereas under differentiation conditions the expression of SOX2 decreased with colony size. The differentiation marker CDX2 showed the opposite trend: a minor population of spontaneously differentiated CDX2$^+$ cells was observed in 1-cell colonies in pluripotent conditions, and the fraction of CDX2$^+$ cells decreased with colony size. By contrast, the fraction of CDX2$^+$ cells increased with colony size when differentiated with BMP4 (Fig. 1E-H, Fig. 3A-C).

Comparing histograms of expression levels for all cells in colonies of a particular size grown under pluripotency conditions, we found a population among 1-cell colonies with reduced SOX2 and enhanced CDX2, and this population was absent from larger colonies (Fig. 3B). This suggests that a fraction of cells spontaneously differentiate to a distinct state and that this differentiation only occurs in colonies with few cells. We also found similar distributions revealing distinct subpopulations of differentiated and undifferentiated 1-cell colonies in differentiation conditions but with the opposite trend: pluripotent cells only persisted in colonies with few cells (Fig. S5A,B). This second population of cells becomes increasingly rare as the colony size increases (Fig. 3C, experimental data). We also confirmed this community effect in a second hESC line (Fig. S5C,D) and that it does not depend on the presence of ROCK inhibitor in the culture medium (Fig. S5E,F).

A simple statistical-mechanical model quantitatively accounts for the community effect

The experiments above show that in the μColony system cells can be in one of two states – pluripotent (SOX2$^+$) or trophectoderm-like (CDX2$^+$). Interactions between cells enforce a common fate inside the colony, while externally supplied BMP4 can bias that common fate towards the CDX2$^+$ state. To explore whether these simple features are sufficient to explain the system’s behavior quantitatively, we exploited an analogy with the Ising model used in statistical physics to describe a two-state system of atomic spins that are coupled to their neighbors and respond to an external field. We made the simplifying assumption that every cell is coupled to every other within a μColony, which is justified by the small colony sizes and the extensive cell movements we observe in the time-lapse experiments below. Within this model, we explored the effects of changing these parameters, and found that increasing either J (the strength of interactions between cells) or the number of cells in the colony will increase the likelihood that all cells in the colony adopt the same fate. As expected, increasing B (the external field corresponding to the BMP4 ligand) leads to a general increase in the fraction of CDX2$^+$ cells, with the transition being gradual at low values of J and sharper at high values (Fig. S6A-C).

To directly compare the model with experimental data, we performed quantitative fitting of the fraction of CDX2$^+$ and SOX2$^+$ cells as a function of colony size using a separate parameter for the value of B and J at each concentration (see Materials and Methods and Fig. S6). The data for the fraction of cells in each subpopulation as a function of colony size at different BMP4 concentrations fit well with this simple model (Fig. 3C, black curves). Further, other

Development (2017) 144, 3042-3053 doi:10.1242/dev.153239

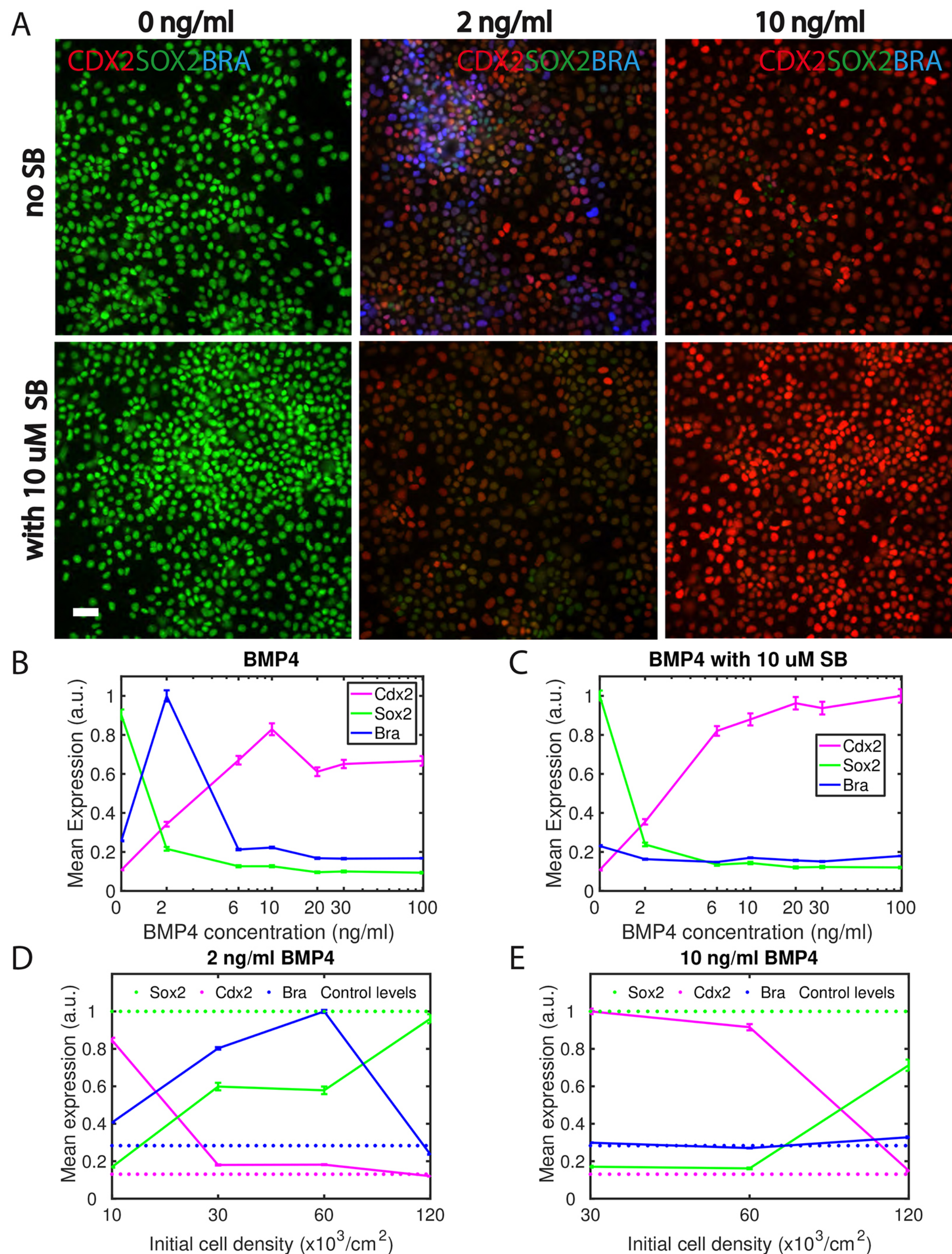

Fig. 2. In standard culture, treatment with BMP4 reveals a morphogen effect that depends on Nodal signaling and cell density. (A) Representative images showing SOX2, CDX2 and BRA marker expression in response to two doses of BMP4. Scale bar: 50 µm. (B,C) Mean expression of SOX2, BRA and CDX2 markers as a function of BMP4 concentrations with (C) and without (B) 10 µm SB431542. The values in B and C are normalized to the maximum over both sets, which were performed in the same experiment. (D,E) Mean expression of SOX2, BRA and CDX2 markers after differentiation with 2 (D) or 10 (E) ng/ml BMP4 with varied initial seeding density. The values in D and E are normalized to the maximum over the two sets, which were performed in the same experiment. Dotted lines represent the levels of expression of the indicated marker under pluripotency conditions. All differentiation experiments were conducted for 42 h. See also Fig. S3. Experiments on dose response to BMP4 in regular culture conditions were performed twice; the density was varied in one experiment. Error bars indicate standard error of the mean over cells.

data not used in fitting the model, such as the distribution of fates within µColonies of a particular size, were predicted by the model without further adjustment to the parameters (Fig. S6D). We also examined the fit values of the parameters B and J as a function of BMP4 concentration (Fig. S6E). As expected, the value of B increased with BMP4 concentration, reflecting the increased bias towards CDX2$^+$ fates. Interestingly, the value of J was nearly constant, reflecting a similar tendency for cells to adopt the same fate within a colony at all BMP4 concentrations. In fact, the data fit equally well with a model in which the value of J was assumed to be the same for all BMP4 concentrations (Fig. S6E).

Taken together, these results suggest that within µColonies BMP4-mediated differentiation can be quantitatively explained by only two features – the bias of differentiation towards the

Development (2017) 144, 3042-3053 doi:10.1242/dev.153239

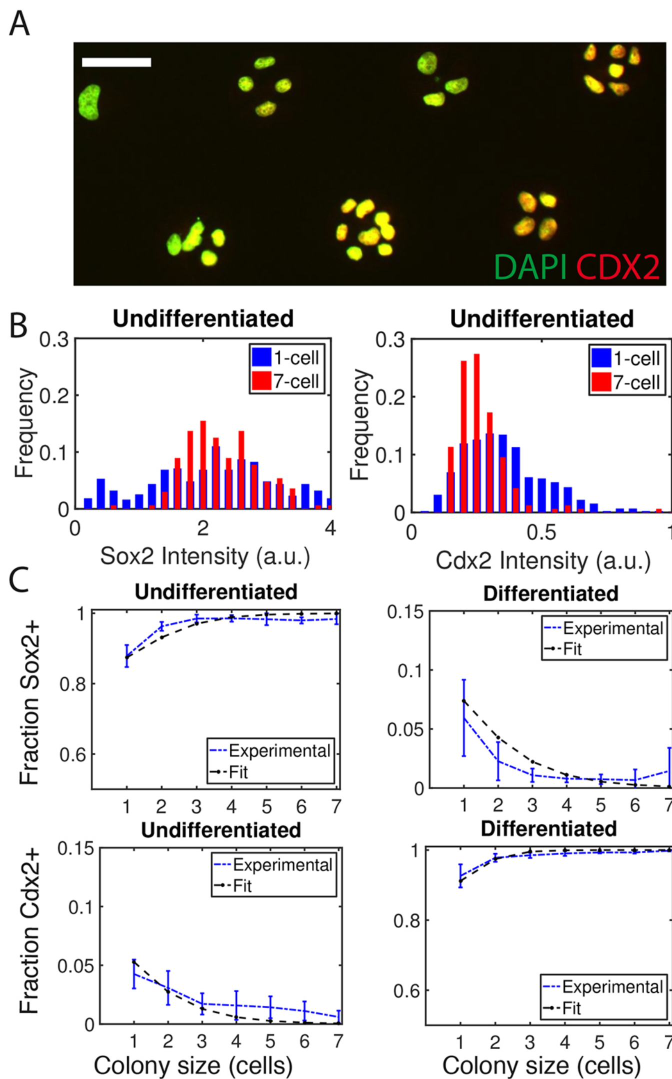

Fig. 3. A community effect enforces a common fate in μColonies. (A) Representative image demonstrating the community effect in differentiated conditions (1 ng/ml BMP4). Scale bar: 50 μm. (B) Distributions of SOX2 and CDX2 expression in cells of 1-cell and 7-cell colonies in undifferentiated conditions. (C) The fraction of cells expressing a given gene is shown with fits to the Ising-like model. Error bars represent s.d. over at least three biological replicates. See also Fig. S5.

trophectoderm-like fate that increases with BMP4 concentration and the constant coupling between neighboring cells that causes them to adopt the same fate.

Proliferation rates and clonal composition do not explain the community effect

A simple hypothesis that would partially explain the observed community effect is that some cells are already differentiated upon seeding. If these cells proliferate more slowly, then we would expect colonies that began with differentiated cells to be on average smaller than those containing pluripotent cells. This hypothesis would predict differences in cell cycle as a function of colony size – that is, cells in smaller colonies would be more likely to be arrested in the G1 phase of the cell cycle. To test this hypothesis, we first analyzed the integrated DAPI intensity as a proxy for the total DNA content of the cells, and found that it did not vary with colony size in either pluripotent or differentiation conditions (Fig. 4A). We next created hESCs expressing RFP-Cdt1, a component of the FUCCI system that is expressed only in G1 phase (Sakaue-Sawano et al., 2008). No differences in the fraction of cells in G1 phase were observed between colonies of different sizes in either pluripotent or differentiation conditions (Fig. 4B). We note that the hypothesis that cell cycle differences underlie the community effect also could not explain our results for the differentiated state, where cells expressing pluripotency markers only persist in small colonies.

To unambiguously establish whether cells within a colony may be more alike because they are clonally derived, we performed an experiment in which we mixed 5% CFP-labeled and 95% unlabeled cells and evaluated their expression of SOX2 in pluripotent conditions or of CDX2 in differentiation conditions. If our results can be explained by the clonal composition of colonies, we would expect that most colonies in our experiments are clonally derived, and that in colonies of mixed clones there are larger differences in the expression of markers such as SOX2 or CDX2 between clones than within the cells of the same clone. In larger colonies of 4-8 cells, colonies with CFP-positive cells frequently had CFP-negative cells as well [61% (8/13) in BMP stimulated; 45% (14/31) in pluripotent conditions], indicating that multiple clones are often present despite the uniformity in CDX2 or SOX2 expression (Fig. 4C). Moreover, quantitatively, within colonies of mixed CFP-positive and CFP-negative cells, the mean CDX2 or SOX2 expression of the CFP-positive and CFP-negative clones were as correlated as for groups of equal numbers of cells chosen randomly without regard to clonal origin (Fig. 4D). Thus, these experiments conclusively exclude clonal expansion as an explanation for the uniformity within a colony in either pluripotency or differentiation. Instead, we favor the interpretation that single cells less robustly interpret the supplied signals than small colonies do (see below), and that signaling enforces uniform differentiation within the colony.

We also investigated whether the community effect could be affected by modulating the pluripotency-maintaining Activin/Nodal and FGF pathways (Fig. S7A,B) or inhibiting the differentiation-promoting Wnt and BMP pathways (Fig. S8), but we did not observe significant differences in the community effect in any of these cases.

Enforcement of sustained signaling during differentiation underlies the community effect in μColonies

To further understand the community effect observed during BMP-mediated differentiation, we generated a reporter cell line for the BMP signaling pathway. We used CRISPR/Cas9 genome engineering to insert GFP at the endogenous locus to form an N-terminal fusion with SMAD4, and isolated a clonal line with a heterozygous insertion of GFP (Fig. S9A-C). Similar fusions have been shown to be faithful reporters of SMAD signaling (Schmierer and Hill, 2005; Sorre et al., 2014; Warmflash et al., 2012). We compared assaying pathway activity with the GFP-SMAD4 reporter and with antibody staining for C-terminally phosphorylated SMAD1/5/8 and found that they give similar dynamics at 1 and 10 ng/ml (Fig. S9D,E).

In undifferentiated cells, GFP-SMAD4 localizes to the cytoplasm and translocates to the cell nucleus upon stimulation with BMP4 (Fig. 5A). We performed live confocal imaging beginning ∼4 h before stimulation and quantified the BMP signaling response by measuring the nuclear to cytoplasmic ratio of GFP-SMAD4 during differentiation induced by 10 ng/ml BMP4 (Fig. 5A,B, Movie 1). To increase statistical power, we seeded reduced numbers of cells in μColonies and focused only on the difference between 1-cell and 2-cell colonies. Note that the designation of number of cells in the

Development (2017) 144, 3042-3053 doi:10.1242/dev.153239

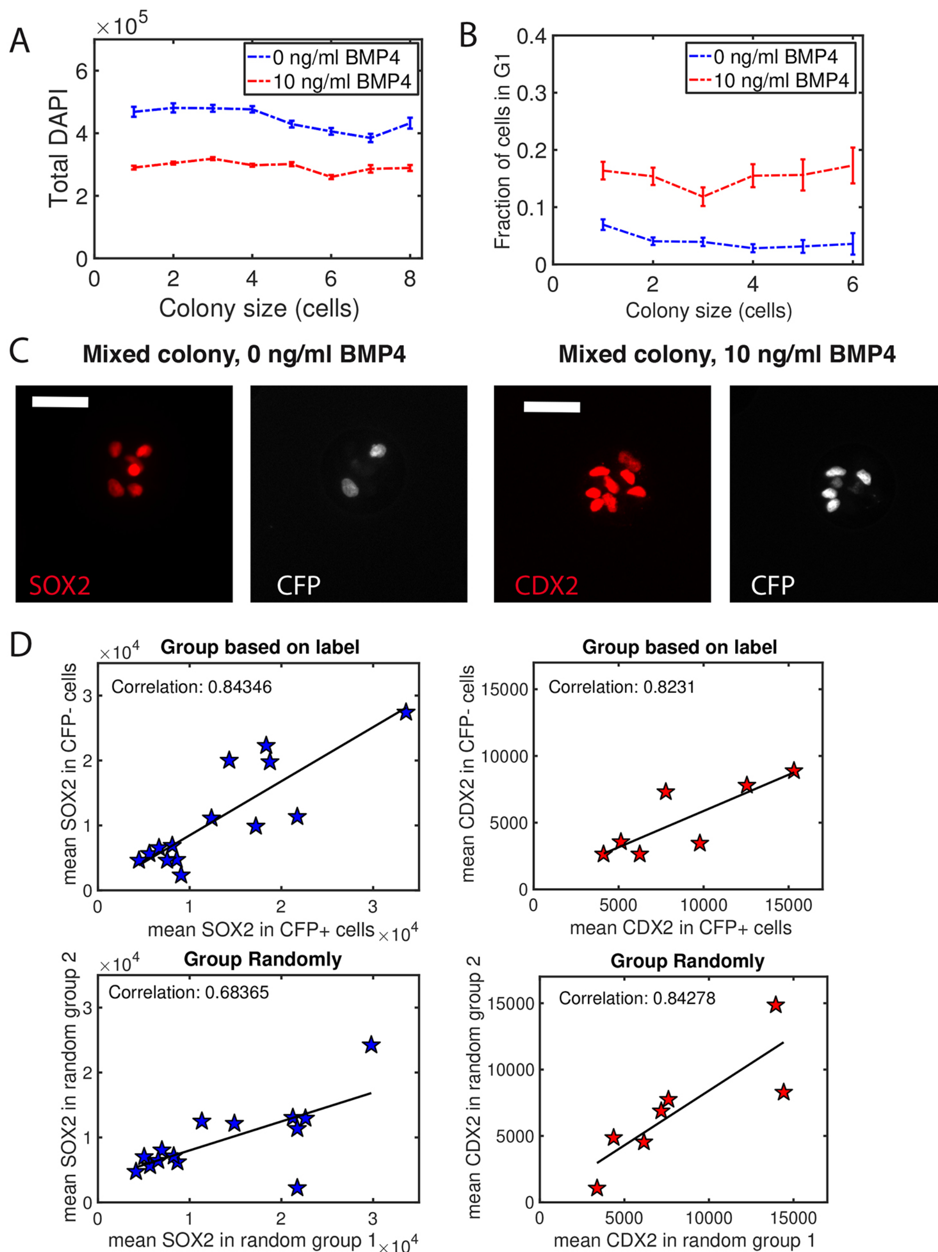

Fig. 4. Neither clonal expansion nor cell cycle effects can explain the community effect. Mean total DNA content (A) and fraction of cells in the G1 phase of the cell cycle (B) as a function of colony size. Error bars represent (A) the s.e.m. calculated separately for each colony size or (B) were calculated using the bootstrapping method. (C) Representative images of μColonies containing both CFP^+ and CFP^- cells in pluripotent or BMP4-treated conditions. Scale bars: 50 μm. (D) Analysis of mean SOX2 or CDX2 levels in the mixed colonies in pluripotent (blue stars) or BMP-treated (red stars) conditions. (Top) 4- to 8-cell colonies containing both CFP^+ and CFP^- cells were identified and the mean SOX2 or CDX2 levels were computed separately for the CFP^+ and the CFP^- cells. (Bottom) In the same mixed colonies, the cells were randomly divided into two groups and the mean levels of SOX2 or CDX2 were computed for each group of cells. The experiment with clonal mixtures of cells in μColonies was performed twice.

colony refers to that at the time of stimulation. We observed both cell division and cell death in colonies of all sizes, and the final number of cells and the number at the time of stimulation will often differ.

The reporter revealed similar signaling intensities in 1-cell and 2-cell colonies before BMP4 stimulation and in the early response to the ligand up to 10 h after stimulation. Thereafter, the mean trajectories began to diverge, with the 2-cell colonies showing higher signaling (Fig. 5C). Examining the distribution of signals in individual cells, we found that this divergence in the mean is mostly due to the presence of 1-cell colonies that revert to near baseline levels of signaling, whereas this does not occur in 2-cell colonies (Fig. 5D-F). Thus, we hypothesized that cells without sustained BMP signaling will fail to differentiate to $CDX2^+$ cells, whereas the high signaling cells will differentiate.

To test this hypothesis directly, we performed live cell imaging of 1-cell colonies, which were then fixed and their levels of CDX2 analyzed. We defined cells as low or high signaling depending on whether their temporal average overlapped with the distribution of signaling before stimulation. We found that 75% of high signaling cells but only 31% of low signaling cells differentiated to a $CDX2^+$ cell fate (Fig. 5H). Differences in the mean signaling intensities between $CDX2^+$ and $CDX2^-$ cells became evident after the early phase of response, similar to the differences between 1-cell and 2-cell colonies (Fig. 5G). To assess whether the cell cycle might play a role in these results, we also examined whether there were differences in cell division depending on whether cells differentiated to a $CDX2^+$ fate. Dividing and non-dividing cells gave rise to $CDX2^+$ cells in approximately equal proportions (Fig. 5I). These data are consistent with a mechanism whereby cell-cell interactions serve to maintain the BMP signaling response, perhaps by directly activating the *BMP4* gene (Karaulanov et al., 2004; Schuler-Metz et al., 2000), and thereby enforce differentiation to trophectoderm-like fates. One-cell colonies that lack this reinforcement both signal and differentiate more heterogeneously.

 Development (2017) 144, 3042-3053 doi:10.1242/dev.153239

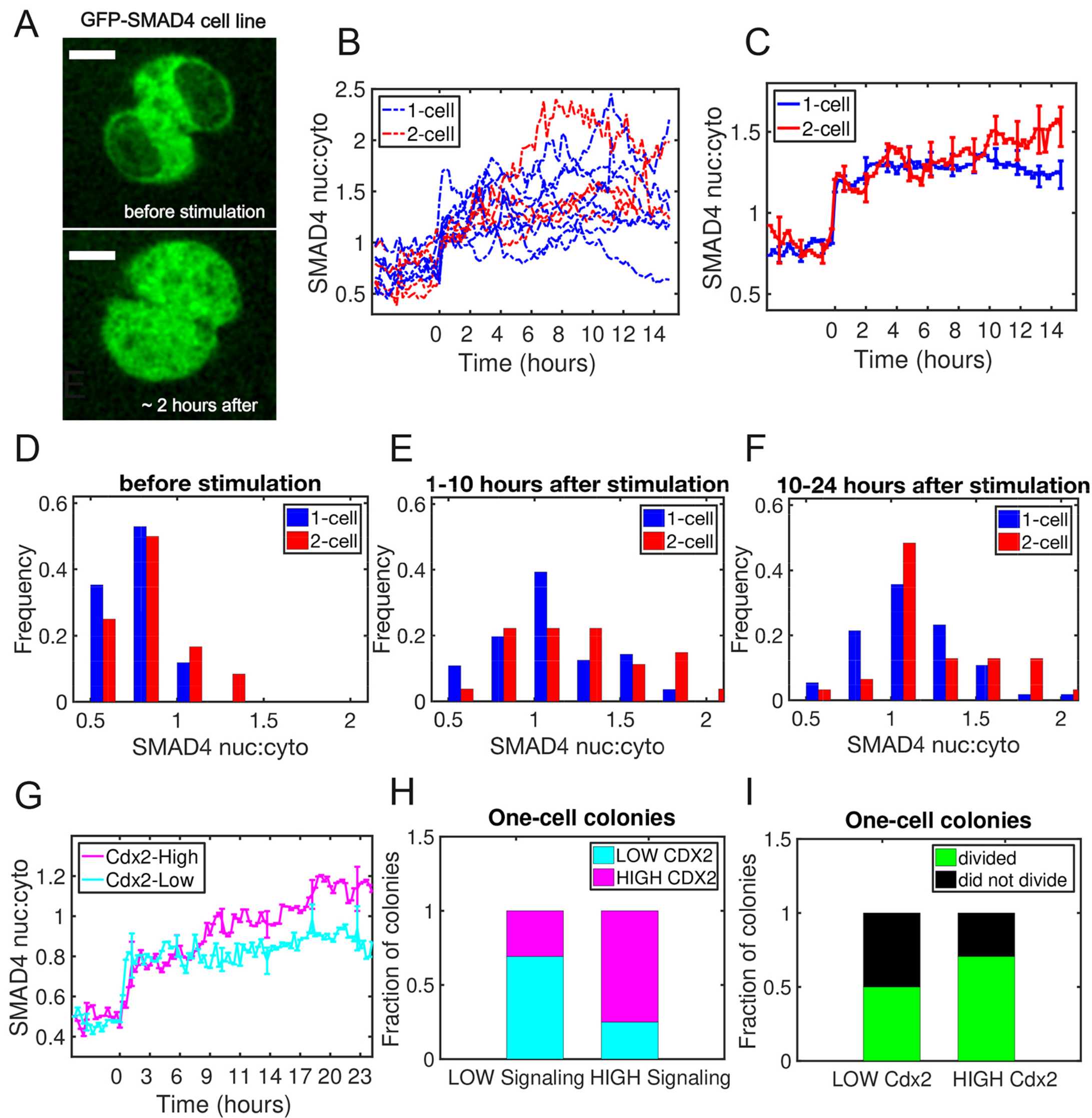

Fig. 5. Reinforcement of the BMP signal underlies the community effect in differentiated cells. (A) Representative images of GFP-SMAD4 reporter cells before and after stimulation with BMP4. Scale bars: 10 µm (see Movie 1). (B) Representative trajectories for the 1-cell and 2-cell colonies treated with 10 ng/ml BMP4. (C) Mean signaling trajectories for 1-cell and 2-cell colonies. (D-F) Mean signaling intensity in individual cells over the indicated time intervals. (G) Cells were classified as high or low expressing for CDX2. The mean signaling is shown in each case. In C and G error bars represent s.e.m. over trajectories. (H) Signaling trajectories were similarly binarized as high or low signaling and the fraction of cells with high or low CDX2 examined as a function of the signaling level. Owing to the difficulty of tracking individual cells for 42 h, cells were fixed and analyzed for CDX2 after 24 h in BMP4. (I) The same colonies from H that contained one cell at the time of BMP4 stimulation were grouped depending on whether that cell later divided and then evaluated for CDX2 expression. Live cell imaging of cells in µColonies and matching of CDX2 levels with signaling were performed twice.

During differentiation in standard culture conditions, sustained signaling is required for differentiation into CDX2⁺ fate

To investigate the relationship between BMP signaling dynamics and differentiation more generally, we performed dose response experiments under standard culture conditions using the same GFP-SMAD4 cell line. At each dose, we measured the BMP signaling dynamics and then fixed the same cells and analyzed their differentiation to $CDX2^+$ trophectoderm-like cells. To avoid the complications of cells adopting multiple fates, we cultured them with SB431542 in order to prevent mesodermal differentiation. Interestingly, in the range of 1-10 ng/ml BMP4, the initial response to ligand stimulation was identical and the trajectories only diverged at later time points, with 1 ng/ml showing significant decay of the signal and 3 ng/ml showing a small decay as compared with cells at 10 ng/ml (Fig. 6A,B top). These trends were mirrored in the differentiation data: cells at 1 ng/ml largely failed to express CDX2, whereas those at 3 ng/ml expressed CDX2 almost as highly as those at 10 ng/ml (Fig. 6B bottom). Since the initial signaling response was the same in all cases, these data demonstrate that the maintenance of signaling, rather than the magnitude of the initial response, is the determining factor for whether cells will differentiate in response to BMP4.

To directly determine whether the initial response or prolonged signaling is responsible for differentiation, we performed experiments in which we treated one group of cells with a high concentration of BMP4 (10 ng/ml) that gave rise to differentiation and another group with a lower dose (1 ng/ml) that did not. After 3 h, we switched the media between these two groups, so that one group was switched from 1 to 10 ng/ml BMP4 while the other was

 Development (2017) 144, 3042-3053 doi:10.1242/dev.153239

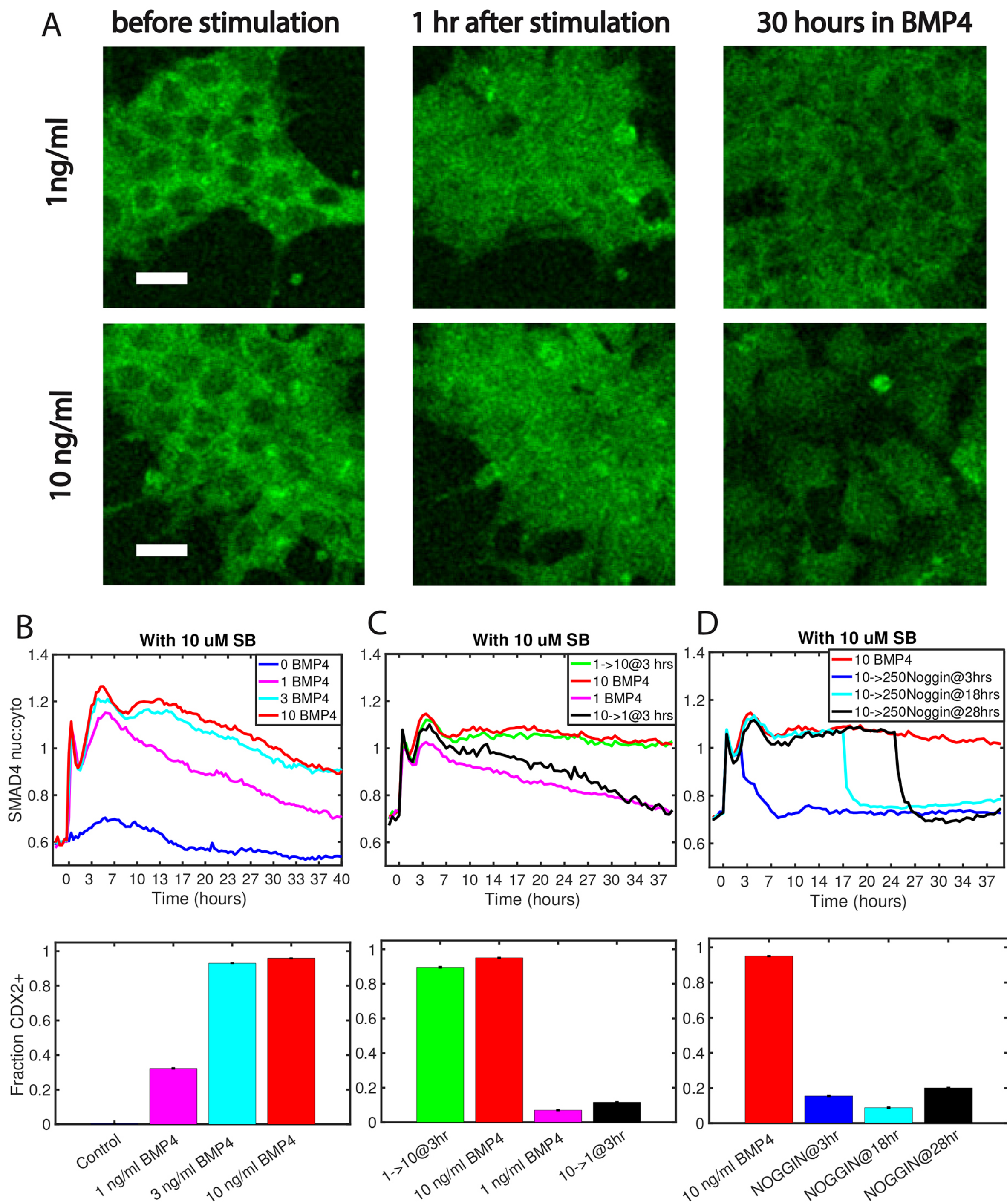

Fig. 6. Cells fates correlate with the duration of signaling rather than the initial response to BMP4. (A) Representative images of GFP-SMAD4 reporter cells in standard culture conditions at the indicated time points following BMP4 treatment. Scale bars: 20 µm. Images were acquired every 20 min. (B-D) (Top) The BMP pathway was stimulated with BMP4 or inhibited with noggin as indicated. The GFP-SMAD4 reporter line was used to determine the signaling activity as a function of time. (Bottom) The same cells were then fixed and analyzed for CDX2 expression. In C, the 1→10 and 10→1 conditions indicate wells that were treated with 1 ng/ml or 10 ng/ml BMP4 and then the medium was swapped between those two wells at 3 h. In D, the 10→250 noggin indicates wells in which the medium containing 10 ng/ml BMP4 was replaced with medium containing 250 ng/ml noggin at the indicated times. Live cell imaging and staining with CDX2 at 1 and 10 ng/ml BMP4 doses were performed twice. Experiments inhibiting signaling with noggin and switching the BMP doses between wells were each performed once.

switched from 10 to 1 ng/ml (Fig. 6C). Consistent with a sustained response being required for differentiation, cells initially stimulated with 10 ng/ml and then switched to 1 ng/ml had a decline in signaling and did not differentiate to $CDX2^+$ fates, whereas those switched from 1 ng/ml to 10 ng/ml had sustained signaling and differentiated. Finally, to directly measure the effect of signal duration on differentiation, we stimulated cells with a high dose (10 ng/ml) of BMP4 and then switched to medium containing the BMP inhibitor noggin (250 ng/ml) at variable times after the initial stimulation. As measured by the GFP-SMAD4 reporter, switching from BMP4-containing medium to noggin-containing medium led to a rapid shutdown of signaling. Importantly, only cells remaining

Development (2017) 144, 3042-3053 doi:10.1242/dev.153239

in BMP4 for 42 h differentiated to $CDX2^+$ fates, whereas those switched to noggin-containing medium at 3, 18 or 28 h failed to differentiate (Fig. 6D).

DISCUSSION

Here we introduce a μColony system that allowed us to separately study exogenous and paracrine signaling in hESCs quantitatively and with cellular resolution. We show that endogenous signals enforce a common fate within the colony, both in pluripotent conditions and when differentiated with BMP4. This enforcement of a common fate allows larger μColonies to respond more robustly to signals supplied in the growth medium: sustaining pluripotency in pluripotency-supporting medium, and differentiating sensitively and homogenously in response to the extrinsic differentiation signal. We show that under standard culture conditions BMP4 acts as a morphogen, inducing different fates in a concentration-dependent manner, whereas in μColonies it switches cells from pluripotency to a single $CDX2^+$ fate, when supplied above a threshold. This apparent discrepancy is due to the need for secondary signals to produce the morphogen effect in standard culture conditions, and μColonies do not reach sufficient densities to produce these secondary signals. We developed a mathematical model that shows that the detailed statistics regarding the number of cells in the pluripotent state or with a trophectoderm-like fate as a function of colony size can be predicted from only two parameters: the strength of the bias towards the trophectoderm-like fates as mediated by BMP4 and the strength of the interactions between cells that enforce a common fate.

The enforcement of a common fate and greater sensitivity to external signals were observed by Gurdon (1988) in the induction of *Xenopus* animal cap cells to muscle fates by vegetal cells, who termed this phenomenon the ‘community effect’. This work showed that individual animal cap cells inserted between two pieces of vegetal tissue failed to differentiate, in contrast to larger aggregates that were induced to muscle fates. This suggested that interactions between the animal cap cells are required to robustly interpret the mesoderm differentiation signals emanating from the vegetal cells. In hESCs, cells at higher density have been shown to better maintain pluripotency upon the withdrawal of pluripotency-maintaining cytokines, also supporting the existence of a community effect promoting this state (Peerani et al., 2007). A related observation has been made regarding the levels of Oct4 and Nanog in colonies of mouse ESCs grown in ‘ground state’ conditions (Muñoz-Descalzo et al., 2012): the levels differ between colonies but are highly similar between cells in the same colony, suggesting reinforcement of common levels through cellular communication. In theoretical work, Bolouri and Davidson (2010) proposed that positive feedback of a signal upon its own transcription could underlie the community effect and applied this idea to the maintenance of the oral ectoderm of the sea urchin embryo through induction of *nodal* gene expression by Nodal signaling. Another theoretical study also found that positive feedback on the signal was sufficient to explain the community effect, and suggested that additional negative feedbacks must operate to prevent the entire tissue from converting to a single fate (Saka et al., 2011). Similarly, in the present study, we find that the enforcement of sustained BMP signaling by interactions between the cells is necessary for ensuring that all cells within the colony adopt the same trophectoderm-like fate.

During development, the community effect serves to ensure a common fate over relatively short length scales, and thereby creates coherent territories of a single cell type. Previous work in hESCs has shown that as colony size is increased, cell fate patterns emerge (Etoc et al., 2016; van den Brink et al., 2014; Warmflash et al., 2014). It is likely that the community effect plays a role in ensuring the coherence of local territories, but other phenomena must emerge on longer length scales to create these patterns. Future work on embryonic patterning with stem cells may probe this transition to understand the emergence of self-organized patterns.

Cells in μColonies of sufficient size differentiate homogenously in response to very low concentrations of ligand. Here, concentrations of 1 ng/ml induced nearly pure populations of $CDX2^+$ $GATA3^+$ trophectoderm-like cells, whereas in larger colonies nearly 100-fold greater concentrations induce a mixture of different fates (Tang et al., 2012; Warmflash et al., 2014). Thus, μColonies seeded at appropriate densities may represent a platform for sensitive and robust directed differentiation.

Our results here suggest that only trophectoderm-like fates are directly induced from hESCs by BMP4, and that it does not directly induce multiple fates in a dose-dependent manner. Experiments involving the inhibition of secondary signals, modulation of cell density, and comparison of μColonies with standard culture establish that there is an apparent morphogen effect in treating hESCs with BMP4, but that this is indirect, relying on secondary signals and only operating at particular cell densities. The role of BMP4 in initiating gastrulation and mesendoderm differentiation both *in vivo* (Winnier et al., 1995) and *in vitro* (Bernardo et al., 2011; Kurek et al., 2015; Warmflash et al., 2014; Yu et al., 2011) requires other signals and was not seen in our experiments at any BMP4 dose in μColonies. Our data suggest that μColonies do not contain sufficient cell numbers to initiate the secondary signals, such as Nodal and Wnt, that operate during gastrulation in the mammalian embryo (Arnold and Robertson, 2009) and are important for patterning pluripotent cells *in vitro* (ten Berge et al., 2008; Warmflash et al., 2014).

It will be interesting to use the methods established here to examine whether these other developmental signaling pathways function directly as morphogens. *In vivo* evidence from genetic perturbations suggests that Nodal signaling induces multiple different fates in a dose-dependent manner during gastrulation (Dunn et al., 2004; Robertson, 2014), and the μColony system could be used to determine whether this is a direct result of cells reading out the Nodal signal or whether other interactions are required. Similarly, as BMP4 has a documented role as a morphogen in dorsal-ventral patterning (Ferguson and Anderson, 1992; Tucker et al., 2008; Wilson et al., 1997), it would be interesting to subject these systems to a similar analysis to determine if cells are directly reading the BMP4 concentration in these cases.

MATERIALS AND METHODS

Routine cell culture

For regular maintenance, hESCs were grown in mTeSR1 (STEMCELL Technologies) in tissue culture dishes coated with Matrigel (Corning; 1:200 in DMEMF12) overnight at 4°C. Cells were passaged using dispase (STEMCELL Technologies) every 3 days. Cells were routinely tested for mycoplasma contamination and found negative. For imaging experiments under standard culture conditions, cells were seeded onto 8- or 4-well imaging slides (ibidi) at densities of ∼63×10^3 cells per cm^2. For density dependence experiments, the densities were varied as indicated.

Micropatterning experiments

We used the micropatterning protocol described in detail by Deglincerti et al. (2016) with adjusted cell numbers. Briefly, micropatterning experiments were performed using HUESM (see Deglincerti et al., 2016) conditioned by mouse embryonic fibroblasts and supplemented with 20 ng/ml bFGF (FGF2; Life Technologies); we refer to this medium as MEF-CM. The

Development (2017) 144, 3042-3053 doi:10.1242/dev.153239

day before seeding onto micropatterns, the medium was switched from mTeSR1 to MEF-CM. The next day, a single-cell suspension was prepared using accutase (Innovative Cell Technologies), and 5.5×10^4 cells in 2 ml MEF-CM with ROCK inhibitor Y27672 (10 µM; StemCell Technologies) were seeded onto the micropatterned coverslip. Custom-patterned glass coverslips (CYTOO) were placed in a 35 mm dish and coated with 2 ml 5 µg/ml laminin-521 (LN521, Biolamina) in DPBS (with calcium and magnesium, Lonza) for 2 h at 37°C. After 2 h, LN521 was washed out by serial dilutions by adding 6 ml DPBS and removing 6 ml (six dilutions). Then, the remaining solution was removed entirely, and cells were placed onto the coverslip and incubated at 37°C. After several hours, the medium was changed and the growth factors or small molecules added as indicated in the text.

Reagents

The following reagents were used to activate or inhibit signaling pathways: BMP4 (R&D Systems; dose as indicated in the text), activin A (R&D Systems; 10 ng/ml), noggin (R&D Systems; 250 ng/ml) lefty A (R&D Systems; 500 ng/ml), SB431542 (Fisher Scientific; 10 µM), PD0325901 (ESI-BIO; 1 µM) LDN-193189 (ESI-BIO; 200 nM), Y27672 (ESI-BIO; 10 µM) and IWP2 (EMD Millipore; 4 µM). When increasing FGF levels, we used bFGF (Life Technologies; 100 ng/ml).

Cell lines

All experiments were performed with the hESC lines ESI017 (purchased from ESI-BIO) or RUES2 (a gift of Ali Brivanlou, Rockefeller University). GFP-SMAD4 reporter cells were made from the parental RUES2 line by CRISPR/Cas9 genome engineering to fuse a cassette containing a puromycin resistance gene (PuroR), a t2a self-cleaving peptide, and GFP onto the N-terminus of SMAD4 so that the locus produces both GFP-SMAD4 and PuroR. Subsequently, cells were nucleofected with an ePiggyBac plasmid containing RFP-H2B driven by the CAG promoter and also containing a blasticidin (Bsd) resistance gene (ePB-B-CAG-RFP-H2B). Cells were selected with 1 µg/ml puromycin and 5 µg/ml Bsd. The RFP-Cdt1 cell line was created by nucleofecting ESI017 cells with an ePiggyBac construct encoding RFP-Cdt1 driven by the CAG promoter and containing a Bsd resistance gene (ePB-B-CAG-RFP-Cdt1). Cells were selected with 5 µg/ml Bsd. The CFP-expressing cells were created by nucleofecting ESI017 cells with an ePiggyBac construct encoding CFP-H2B driven by the CAG promoter and containing a neomycin resistance gene (ePB-N-CAG-CFP-hH2B). Cells were selected with 200 µg/ml G418.

Immunostaining

Coverslips were rinsed with DPBS, fixed for 20 min in 4% paraformaldehyde, rinsed twice with DPBS, and blocked for 30 min at room temperature. The blocking solution contained 3% donkey serum and 0.1% Triton X-100 in 1× DPBS. After blocking, the cells were incubated with primary antibodies at 4°C overnight (Table S1). The next day, the cells were washed three times with DPBST (1× DPBS with 0.1% Tween 20) and incubated with secondary antibodies (AlexaFluor 488 A21206, AlexaFluor 555 A31570 and A21432, and AlexaFluor 647 A31571, ThermoFisher; 1:500) and DAPI for 30 min at room temperature. After secondary antibody treatment, samples were washed twice in DPBST at room temperature. Coverslips were then mounted in Fluoromount-G (Southern Biotech) and allowed to dry for several hours.

Imaging

Entire fixed coverslips were imaged using tiled acquisition with a 20×, NA 0.75 objective on an Olympus IX83 inverted epifluorescence microscope. For live cell imaging, RUES2-GFP-SMAD4/RFP-H2B reporter cells were seeded on the micropattern as described above and the patterned coverslip was then moved into a holder (CYTOO) to allow for imaging through the coverslip without any intervening material. Images were acquired on an Olympus/Andor spinning disk confocal microscope with either a 40×, NA 1.25 silicon oil objective or a 60×, NA 1.35 oil objective. Approximately four *z*-planes were acquired at each position every 12-17 min. For live cell imaging in standard culture conditions, reporter cells were seeded onto ibidi slides as described above and imaged on an Olympus FV12 laser scanning confocal microscope with a 20×, NA 0.75 objective at intervals of 20 min. We typically acquired 2-4 h of data before BMP4 stimulation and subsequently 20-24 h for µColonies and 40 h for standard culture conditions.

Image analysis

Fixed cell experiments utilized large tiled images that were computationally separated into smaller images of 2048×2048 pixels. As the boundaries of these smaller images do not align exactly with the individual images as originally acquired and stitched together by the acquisition software, images presented may derive from one to four individual camera acquisitions. Images of fixed cells acquired at 20× on the epifluorescence microscope were segmented using custom software written in MATLAB (MathWorks) as described previously (Warmflash et al., 2012, 2014). Identified cells were grouped into µColonies based on the distance to their neighbors. Cells within 80 µm were considered to be within a single µColony. We visually inspected colony groupings for accuracy. Mean fluorescence intensities for each cell were quantified and intensities for markers were normalized to the mean intensity of the DAPI stain in each cell. All averages are taken over at least 100 cells in µColonies or over at least 2000 cells in regular culture conditions. Images from live cell experiments were first processed in ilastik (http://ilastik.org) to create nuclear and cellular masks. Custom MATLAB software was used to postprocess these masks to separate touching cells and to quantify both nuclear and cytoplasmic intensities.

Cell-cell communication model

In the conventional Ising model, the energy of a system of atoms in an external magnetic field B can be written as a sum of energy due to interactions between the neighboring spins and the energy due to the magnetic field:

$$H = H_B + H_J = -B\sum_{i}^{N} s_i - \frac{J}{2}\sum_{i,j}^{N} s_i s_j. \quad (1)$$

The probability P for the system to be in state σ is given by Boltzman distribution:

$$P(\sigma) = \frac{e^{-\beta H(\sigma)}}{Z} \quad (2)$$

$$Z = \sum_{\sigma} e^{-\beta H(\sigma)}, \quad (3)$$

where Z is the partition function of the system representing the sum of probabilities of all possible states and β is the inverse temperature given by $1/\kappa_B$T. Here, we reinterpret this energy to represent a system of interacting cells exposed to an external ligand. The indices *i* and *j* run over all cells in the colony, and the variable s_i is 1 if the *i*th cell is in the $CDX2^+$ state and −1 if the cell is in the $SOX2^+$ state.

Note from the equations defining the model (1-3), that only products βB and βJ appear so that we are free to choose units of energy such that β is equal to 1. We consider a system of size N cells, where the external field B quantifies BMP4 concentration and the parameter J quantifies the strength of the interactions between cells. If the parameter J>0, this interaction favors configurations in which neighboring cells have the same identity. We make the simplifying assumption that all cells in the µColony are neighbors, which is justified by the small sizes of the µColonies and the extensive cell rearrangements that occur during the observation period (see Movie 1). If we take n cells to be in the $CDX2^+$ state favored by the field B, then (N-n) cells are in the $SOX2^+$ state and the portion of the energy due to external ligand is given by:

$$H_B = -(Bn - (N-n)B) = -(2n - N)B. \quad (4)$$

The energy due to cell-cell interactions will be given by:

$$H_J = -J/2\{n(n-1)/2 + (N-n-1)(N-n)/2 - n(N-n)\}, \quad (5)$$

where the first two terms in the sum represent the pairs of interacting cells, which are in the same state ($SOX2^+$ or $CDX2^+$) and are energetically

favorable. The last term represents the interactions between the $SOX2^+$ and $CDX2^+$ cells that are energetically unfavorable.

The total non-normalized probability for the μColony to have n cells in $CDX2^+$ state and (N-n) cells in $SOX2^+$ state is then:

$$P(n,N) = C_n^N e^{B(2n-N)} e^{J/2((N-2n)^2-N)}, \quad (6)$$

where C_n^N represents the number of combinations of n out of N $(C_n^N = N!)/(n!(N-n)!)$.

The partition function Z is given by:

$$Z = \sum_{states} P(n,N) = \sum_{n=0}^{N} C_n^N e^{B(2n-N)} e^{J/2((N-2n)^2-N)}. \quad (7)$$

These probabilities are then used to compute averages. For the results in Fig. 3, the average fraction of cells in the $CDX2^+$ state is:

$$f = \sum_{n=0}^{N} (n/N) \frac{P(n,N)}{Z}. \quad (8)$$

To obtain the theoretical predictions to be compared with the experimental data, we repeated this calculation for all values of N. We then minimized the sum of squared differences between the model predictions and the data using a Monte-Carlo minimization algorithm coded in MATLAB. We performed this fitting independently for each value of the BMP4 concentration, and also performed a fit to all the data in which the value of J was fixed to be the same for all BMP4 concentrations, but the value of B at each concentration was considered a separate parameter (see Fig. S6E).

Acknowledgements
We thank Ali Brivanlou for providing the RUES2-GFP-SMAD4 cell line and the ePB-B-CAG-RFP-Cdt1 plasmid, Eric Siggia and Daniel Wagner for comments on the manuscript, and members of the A.W. lab for helpful discussions and feedback.

Competing interests
The authors declare no competing or financial interests.

Author contributions
Conceptualization: A.N., A.W.; Methodology: A.N., I.H., A.W.; Software: A.N., I.H., A.W.; Formal analysis: A.N., I.H., A.W.; Investigation: A.N.; Resources: A.R.; Writing - original draft: A.N., A.W.; Writing - review & editing: A.N., A.W.; Visualization: A.N., A.R., A.W.; Supervision: A.W.; Project administration: A.W.; Funding acquisition: A.W.

Funding
This work was supported by Rice University and grants to A.W. from the National Science Foundation (MCB-1553228), the Cancer Prevention and Research Institute of Texas (RR 140073), and the John S. Dunn Foundation.

Data availability
Custom-written MATLAB codes for image segmentation and cell tracking of μColonies can be found on GitHub in repository warmflasha/CellTracker (https://github.com/warmflasha/CellTracker).

Supplementary information
Supplementary information available online at
http://dev.biologists.org/lookup/doi/10.1242/dev.153239.supplemental

References

Arnold, S. J. and Robertson, E. J. (2009). Making a commitment: cell lineage allocation and axis patterning in the early mouse embryo. *Nat. Rev. Mol. Cell Biol.* **10**, 91-103.
Bernardo, A. S., Faial, T., Gardner, L., Niakan, K. K., Ortmann, D., Senner, C. E., Callery, E. M., Trotter, M. W., Hemberger, M., Smith, J. C. et al. (2011). BRACHYURY and CDX2 mediate BMP-induced differentiation of human and mouse pluripotent stem cells into embryonic and extraembryonic lineages. *Cell Stem Cell* **9**, 144-155.
Bier, E. and De Robertis, E. M. (2015). EMBRYO DEVELOPMENT. BMP gradients: a paradigm for morphogen-mediated developmental patterning. *Science* **348**, aaa5838.
Bolouri, H. and Davidson, E. H. (2010). The gene regulatory network basis of the "community effect," and analysis of a sea urchin embryo example. *Dev. Biol.* **340**, 170-178.
Deglincerti, A., Etoc, F., Guerra, M. C., Martyn, I., Metzger, J., Ruzo, A., Simunovic, M., Yoney, A., Brivanlou, A. H., Siggia, E. et al. (2016). Self-organization of human embryonic stem cells on micropatterns. *Nat. Protoc.* **11**, 2223-2232.
Dunn, N. R., Vincent, S. D., Oxburgh, L., Robertson, E. J. and Bikoff, E. K. (2004). Combinatorial activities of Smad2 and Smad3 regulate mesoderm formation and patterning in the mouse embryo. *Development* **131**, 1717-1728.
Etoc, F., Metzger, J., Ruzo, A., Kirst, C., Yoney, A., Ozair, M. Z., Brivanlou, A. H. and Siggia, E. D. (2016). A balance between secreted inhibitors and edge sensing controls gastruloid self-organization. *Dev. Cell* **39**, 302-315.
Ferguson, E. L. and Anderson, K. V. (1992). Decapentaplegic acts as a morphogen to organize dorsal-ventral pattern in the Drosophila embryo. *Cell* **71**, 451-461.
Gurdon, J. B. (1988). A community effect in animal development. *Nature* **336**, 772-774.
Horii, M., Li, Y., Wakeland, A. K., Pizzo, D. P., Nelson, K. K., Sabatini, K., Laurent, L. C., Liu, Y. and Parast, M. M. (2016). Human pluripotent stem cells as a model of trophoblast differentiation in both normal development and disease. *Proc. Natl. Acad. Sci. USA* **113**, E3882-E3891.
Karaulanov, E., Knöchel, W. and Niehrs, C. (2004). Transcriptional regulation of BMP4 synexpression in transgenic Xenopus. *EMBO J.* **23**, 844-856.
Kurek, D., Neagu, A., Tastemel, M., Tüysüz, N., Lehmann, J., van de Werken, H. J. G., Philipsen, S., van der Linden, R., Maas, A., van IJcken, W. F. J. et al. (2015). Endogenous WNT signals mediate BMP-induced and spontaneous differentiation of epiblast stem cells and human embryonic stem cells. *Stem Cell Rep.* **4**, 114-128.
Li, Y. and Parast, M. M. (2014). BMP4 regulation of human trophoblast development. *Int. J. Dev. Biol.* **58**, 239-246.
Li, Y., Moretto-Zita, M., Soncin, F., Wakeland, A., Wolfe, L., Leon-Garcia, S., Pandian, R., Pizzo, D., Cui, L., Nazor, K. et al. (2013). BMP4-directed trophoblast differentiation of human embryonic stem cells is mediated through a ΔNp63+ cytotrophoblast stem cell state. *Development* **140**, 3965-3976.
Muñoz-Descalzo, S., Rué, P., Garcia-Ojalvo, J. and Martinez Arias, A. (2012). Correlations between the levels of Oct4 and Nanog as a signature for naïve pluripotency in mouse embryonic stem cells. *Stem Cells* **30**, 2683-2691.
Peerani, R., Rao, B. M., Bauwens, C., Yin, T., Wood, G. A., Nagy, A., Kumacheva, E. and Zandstra, P. W. (2007). Niche-mediated control of human embryonic stem cell self-renewal and differentiation. *EMBO J.* **26**, 4744-4755.
Robertson, E. J. (2014). Dose-dependent Nodal/Smad signals pattern the early mouse embryo. *Semin. Cell Dev. Biol.* **32**, 73-79.
Saka, Y., Lhoussaine, C., Kuttler, C., Ullner, E. and Thiel, M. (2011). Theoretical basis of the community effect in development. *BMC Syst. Biol.* **5**, 54.
Sakaue-Sawano, A., Kurokawa, H., Morimura, T., Hanyu, A., Hama, H., Osawa, H., Kashiwagi, S., Fukami, K., Miyata, T., Miyoshi, H. et al. (2008). Visualizing spatiotemporal dynamics of multicellular cell-cycle progression. *Cell* **132**, 487-498.
Schmierer, B. and Hill, C. S. (2005). Kinetic analysis of Smad nucleocytoplasmic shuttling reveals a mechanism for transforming growth factor beta-dependent nuclear accumulation of Smads. *Mol. Cell. Biol.* **25**, 9845-9858.
Schuler-Metz, A., Knöchel, S., Kaufmann, E. and Knöchel, W. (2000). The homeodomain transcription factor Xvent-2 mediates autocatalytic regulation of BMP-4 expression in Xenopus embryos. *J. Biol. Chem.* **275**, 34365-34374.
Sorre, B., Warmflash, A., Brivanlou, A. H. and Siggia, E. D. (2014). Encoding of temporal signals by the TGF-β pathway and implications for embryonic patterning. *Dev. Cell* **30**, 334-342.
Tang, C., Ardehali, R., Rinkevich, Y., Seita, J., Lee, A. S., Mosley, A. R., Drukker, M., Weissman, I. L. and Soen, Y. (2012). isolation of primitive endoderm, mesoderm, vascular endothelial and trophoblast progenitors from human pluripotent stem cells. *Nat. Biotechnol.* **30**, 531-542.
ten Berge, D., Koole, W., Fuerer, C., Fish, M., Eroglu, E. and Nusse, R. (2008). Wnt signaling mediates self-organization and axis formation in embryoid bodies. *Cell Stem Cell* **3**, 508-518.
Tucker, J. A., Mintzer, K. A. and Mullins, M. C. (2008). The BMP signaling gradient patterns dorsoventral tissues in a temporally progressive manner along the anteroposterior axis. *Dev. Cell* **14**, 108-119.
van den Brink, S. C., Baillie-Johnson, P., Balayo, T., Hadjantonakis, A.-K., Nowotschin, S., Turner, D. A. and Martinez Arias, A. (2014). Symmetry breaking, germ layer specification and axial organisation in aggregates of mouse embryonic stem cells. *Development* **141**, 4231-4242.
Warmflash, A., Zhang, Q., Sorre, B., Vonica, A., Siggia, E. D. and Brivanlou, A. H. (2012). Dynamics of TGF-β signaling reveal adaptive and pulsatile behaviors reflected in the nuclear localization of transcription factor Smad4. *Proc. Natl. Acad. Sci. USA* **109**, E1947-E1956.
Warmflash, A., Sorre, B., Etoc, F., Siggia, E. D. and Brivanlou, A. H. (2014). A method to recapitulate early embryonic spatial patterning in human embryonic stem cells. *Nat. Methods* **11**, 847-854.
Wilson, P. A., Lagna, G., Suzuki, A. and Hemmati-Brivanlou, A. (1997). Concentration-dependent patterning of the Xenopus ectoderm by BMP4 and its signal transducer Smad1. *Development* **124**, 3177-3184.
Winnier, G., Blessing, M., Labosky, P. A. and Hogan, B. L. (1995). Bone morphogenetic protein-4 is required for mesoderm formation and patterning in the mouse. *Genes Dev.* **9**, 2105-2116.

Development (2017) 144, 3042-3053 doi:10.1242/dev.153239

Xu, R.-H., Chen, X., Li, D. S., Li, R., Addicks, G. C., Glennon, C., Zwaka, T. P. and Thomson, J. A. (2002). BMP4 initiates human embryonic stem cell differentiation to trophoblast. *Nat. Biotechnol.* **20**, 1261-1264.

Yu, P., Pan, G., Yu, J. and Thomson, J. A. (2011). FGF2 sustains NANOG and switches the outcome of BMP4-induced human embryonic stem cell differentiation. *Cell Stem Cell* **8**, 326-334.

DEVELOPMENT